Research Article

An investigation on responses of thermoelastic interactions of transversely isotropic thick circular plate due to ring load with memory-dependent derivatives

Iqbal Kaur[1] · **Kulvinder Singh**[2]

Received: 29 November 2022 / Accepted: 27 February 2023
Published online: 22 March 2023

Abstract
The present investigation has focus on the variations in a transversely isotropic thick circular plate subjected to ring loading. The modified Green Nagdhi (GN) heat conduction equation with and without energy dissipation by introducing memory-dependent derivatives (MDD) with two temperatures has been used to model the problem. General solutions to the field equations have been found using the Hankel and Laplace transform. The analytical expressions of stress, conductive temperature, and components of displacement are obtained in the transformed domain. Physical solutions have been obtained using numerical inversion techniques. The effects of Kernel functions of memory-dependent derivatives have been depicted graphically. The present investigation also reveals some specific cases.

Article highlights

- A novel mathematical model of transversely isotropic thick circular plate with modified GN-III heat conduction equation with MDD is presented.
- The medium is exposed to ring load at its boundary surface.
- Dynamic response of Kernel functions of memory-dependent derivatives is investigated.
- The effects of memory-dependent derivatives with two temperatures on all physical fields are studied and illustrated graphically.

Keywords Memory dependent derivatives · Transversely isotropic · Kernel functions · Hankel transform · Thick circular plate · Ring load · Laplace transform

List of symbols

e_{ij}	Strain tensors
$\vec{u}$	Displacement vector
K_{ij}^{*}	Materialistic constant
α_{ij}	Linear thermal expansion coefficient
$\delta(t)$	Dirac's delta function
χ	Time delay
τ_0	Relaxation time
t_{ij}	Stress tensors
δ_{ij}	Kronecker delta
u_i	Components of displacement
a_{ij}	Two temperature parameters
C_E	Specific heat
x_i	Position vector
β_{ij}	Thermal elastic coupling tensor
C_{ijkl}	Elastic parameters
φ	Conductive temperature
t	Time
T_0	Reference temperature
T	Absolute temperature

✉ Iqbal Kaur, bawahanda@gmail.com; Kulvinder Singh, ksingh2015@kuk.ac.in | [1]Department of Mathematics, Government College for Girls, Palwal, Kurukshetra, India. [2]Faculty of Engineering, UIET, Kurukshetra University, Kurukshetra, Haryana, India.

C_1 Longitudinal wave velocity
ρ Medium density
K_{ij} Thermal conductivity

1 Introduction

Classical elasticity theory focuses on stress and strain distributions developed in elastic bodies when forces are applied or temperatures change. As temperature changes, results in thermal effects on the material, such as thermal strain, deformation, and thermal stress. The coupled theory of thermoelasticity arises from the coupling between the thermal and strain fields. A temperature gradient in an elastic medium coupled with strain distribution was first studied by Duhamel [1]. Based on this theory, numerous researchers have solved several interesting problems. Sharma et al. [2] studied a homogeneous transversely isotropic thermoelastic (HTIT) material with two temperatures w.r.t. Green-Naghdi-II theory to illustrate the 2-D deformation using Laplace and Fourier transforms. With the help of Laplace and Hankel transforms, Kumar et al. [3] investigated the thermomechanical behavior of a homogeneous isotropic thick plate with an axisymmetric heat supply. The thermoelastic diffusion interactions in a thick circular copper material plate were presented by Tripathi et al. [4]. The thermoelastic effect on an infinitely extended thick plate with an axisymmetric temperature distribution was studied by Kant and Mukhopadhyay [5]. Using generalized thermoelasticity based on memory-dependent axisymmetric temperature distributions, Kant and Mukhopadhyay [6] analyzed the thermoelastic effects of an infinitely extended thick plate with axisymmetric temperature distribution. Youssef [7] discussed the thermoelastic behavior without energy dissipation with linear theory of thermoelasticity. Considering two-temperature thermoelasticity theory in the frequency domain, Lata [8] investigated the thermomechanical interactions in the fractional theory of thermoelasticity on a homogeneous, isotropic thick circular plate. With both plasmaelastic (PE) and thermoelastic (TE) wave impacts, theoretical models of optically induced elastic bending for a semiconductor circular plate (clamped and simply supported) were developed by Galović et al. [9].

A modified version of the Mindlin theory of motion is offered by Senjanović et al. [10] for rotations and total deflection. To analyse the vibration of circular plates, the governing equations are converted from an orthogonal to a polar coordinate system. The flexural vibration fourth-order differential equations are further divided into two second-order Bessel-type equations. To analyse how porosity, phase delays, one relaxation period, and the couple stress parameter respond, the thick circular plate problem in the modified coupled stress theory (MCST) with voids model is investigated by Kumar et al. [11]. The eigenvalue approach in a homogeneous, isotropic, non-local micro-stretch thermoelastic circular plate has been studied by Kumar et al. [12]. On the obtained numbers, the effects of non-locality, both with and without energy dissipation, are examined numerically and graphically. Kaur and Singh [13] focused on developing a mathematical model to analyze fluctuations in fractional order strain (FoS) in transversely isotropic, homogeneous circular plates with ring loads, hyperbolic two temperatures (H2T), and energy dissipation. The generic solution to the field equations has been discovered using the Laplace and Hankel transform. Mallik and Kanoria [14] studied a two-dimensional thick, transversely isotropic plate with a heat source, while the lower surface of the plate rests on a hard foundation and is thermally insulated, the top surface of the plate is stress-free and has a predetermined surface temperature. Hasheminejad and Rafsanjani [15] reported a precise 3-D study for the steady-state dynamic response of an arbitrarily thick, isotropic, and functionally graded plate strip. This study was caused by the action of a transverse distributed moving line load propagating parallel to the infinite simply supported edges of the plate strip at constant speed. Kaur and Singh[16, 17] discussed the MDD in nano-beams. Some other researchers also worked on similar research on MDD or semiconductor medium as, Nasr et al. [18], Abouelregal et al. [19], Abouelregal et al. [20].

The MDD is better suited for temporal remodelling than the fractional order derivative. It exhibits the memory effect more clearly. A better MDD model of thermoelasticity was introduced to show the memory effect (the rate of sudden change depends on the past state). MDD is defined in an integral form of a common derivative with a kernel function on a slip-in interval. A common derivative and kernel function is used to define the MDD in integral form. In many models that explain physical terms with the memory effect, the kernels in physical laws are crucial. Ezzat et al. [21] studied the thermo-viscoelasticity with MDD. Ezzat et al. [22, 23] discussed the MDD in magneto-thermoelasticity and thermoelasticty with two temperatuer.

The primary goal of the current work is to use memory-dependent derivatives to examine the deformity in a transversely isotropic thick circular plate with ring load due to thermal and mechanical sources. The heat conduction equation depending on the memory-dependent derivative is developed in Sect. 2 along with the formulation of the governing equations for the GN-III theory of thermoelasticity. Four alternative kernel functions, one of which is non-linear in nature, have been taken into consideration. A thick plate is taken into consideration as part of the formulation of the problem in Sect. 3, the Laplace and Hankel

transform to solve the issue, and the results are produced in the transformed domain. Section 4 described the boundary conditions. Section 5 presents the application of the problem. However, the resulting quantities are achieved in the physical domain by utilizing the numerical inversion technique in Sect. 6. Some particular cases are also figured out from the present investigation as mentioned in Sect. 7. Section 8 provides a full explanation of the numerical findings and discussion of the current study, as well as comparisons of each physical field for various kernels. To highlight the key findings, Sect. 9 summarises the present work's conclusion.

2 Basic equations

The constitutive relations for an anisotropic thermoelastic media are as follows:

$$t_{ij} = C_{ijkl}e_{kl} - \beta_{ij}T \tag{1}$$

$$C_{ijkl}e_{kl,j} - \beta_{ij}T_{,j} = \rho\ddot{u}_i \tag{2}$$

Modified Heat Conduction equation with MDD and GN-III theory following Green and Naghdi [24] and Wang and Li [25] is

$$K_{ij}\varphi_{,ij} + K^*_{ij}\dot{\varphi}_{,ij} = \left(1 + \chi D_\chi\right)\left(\beta_{ij}T_0\ddot{e}_{ij} + \rho C_E\ddot{T}\right) \tag{3}$$

where

$$T = \varphi - a_{ij}\varphi_{,ij}, \tag{4}$$

$$\beta_{ij} = C_{ijkl}\alpha_{kl}, \tag{5}$$

$$e_{ij} = \frac{1}{2}\left(u_{i,j} + u_{j,i}\right), \quad i,j = 1,2,3. \tag{6}$$

Here $C_{ijkl}\left(C_{ijkl} = C_{klij} = C_{jikl} = C_{ijlk}\right)$.

First-order MDD for a differentiable function f(t) for a fixed time t with delay $\chi > 0$ is given as:

$$D_\chi f(t) = \frac{1}{\chi}\int_{t-\chi}^{t} K(t-\xi)f'(\xi)d\xi,$$

The choice of the $K(t-\xi)$ and χ are determined by the material properties [26]. The kernel function $K(t-\xi)$ is written as:

$$K(t-\xi) = 1 - \frac{2\beta}{\chi}(t-\xi) + \frac{\alpha^2}{\chi^2}(t-\xi)^2 = \begin{cases} 1 & \alpha = 0, \beta = 0, \\ 1 + (\xi - t)/\chi & \alpha = 0, \beta = 1/2, \\ \left[1 + (\xi - t)/\chi\right]^2 & \alpha = 1, \beta = 1. \end{cases}$$

where α and β are constants. Additionally, the comma indicates the derivative w. r. t. the space variable and the dot superimposed on it signifies the time derivative.

3 Formulation of the problem

Suppose that a transversely isotropic thick circular plate occupies the space defined by $0 \le r \le \infty, -b \le z \le b$, with a ring load of thickness 2b. Axisymmetric heat supply should be applied to the plate in both the radial and axial directions. Heat flux $g_0F(r,z)$ is prescribed on the upper and lower surfaces of the thick circular plate with ring load at a constant temperature T_0. For this problem, we take a cylindrical polar coordinate system (r,θ,z) symmetric around the *Z-axis*. Our analysis is restricted to two dimensions due to the plane-axisymmetric nature of the problem, which means the field component $(v = 0)$ and $(u, w, \text{ and } \varphi)$ is independent of θ. In addition, using Slaughter [27] on (1)–(3), we obtain the equations for transversely isotropic thermoelastic solids with two temperatures and no energy dissipation by following the appropriate transformation.

$$C_{11}\left(\frac{\partial^2 u}{\partial r^2} + \frac{1}{r}\frac{\partial u}{\partial r} - \frac{1}{r}u\right) + C_{13}\left(\frac{\partial^2 w}{\partial r \partial z}\right) + C_{44}\frac{\partial^2 u}{\partial z^2} + C_{44}\left(\frac{\partial^2 w}{\partial r \partial z}\right) - \beta_1\frac{\partial}{\partial r}\left\{\varphi - a_1\left(\frac{\partial^2\varphi}{\partial r^2} + \frac{1}{r}\frac{\partial\varphi}{\partial r}\right) - a_3\frac{\partial^2\varphi}{\partial z^2}\right\} = \rho\frac{\partial^2 u}{\partial t^2}, \tag{7}$$

$$\left(C_{11} + C_{44}\right)\left(\frac{\partial^2 u}{\partial r \partial z} + \frac{1}{r}\frac{\partial u}{\partial z}\right) + C_{44}\left(\frac{\partial^2 w}{\partial r^2} + \frac{1}{r}\frac{\partial w}{\partial r}\right) + C_{33}\frac{\partial^2 w}{\partial z^2} - \beta_3\frac{\partial}{\partial z}\left\{\varphi - a_1\left(\frac{\partial^2\varphi}{\partial r^2} + \frac{1}{r}\frac{\partial\varphi}{\partial r}\right) - a_3\frac{\partial^2\varphi}{\partial z^2}\right\} = \rho\frac{\partial^2 w}{\partial t^2}, \tag{8}$$

$$\left(K_1 + K_1^*\frac{\partial}{\partial t}\right)\left(\frac{\partial^2\varphi}{\partial r^2} + \frac{1}{r}\frac{\partial\varphi}{\partial r}\right) + \left(K_3 + K_3^*\frac{\partial}{\partial t}\right)\frac{\partial^2\varphi}{\partial z^2} = \left(1 + \chi D_\chi\right)\left[T_0\frac{\partial^2}{\partial t^2}\left(\beta_1\frac{\partial u}{\partial r} + \beta_3\frac{\partial w}{\partial z}\right) + \rho C_E\frac{\partial^2}{\partial t^2}\left\{\varphi - a_1\left(\frac{\partial^2\varphi}{\partial r^2} + \frac{1}{r}\frac{\partial\varphi}{\partial r}\right) - a_3\frac{\partial^2\varphi}{\partial z^2}\right\}\right]. \tag{9}$$

Constitutive relations for the transversely isotropic medium are

$$t_{rr} = C_{11}e_{rr} + C_{12}e_{\theta\theta} + C_{13}e_{zz} - \beta_1 T, \tag{10}$$

$$t_{zr} = 2C_{44}e_{rz}, \tag{11}$$

$$t_{zz} = C_{13}e_{rr} + C_{13}e_{\theta\theta} + C_{33}e_{zz} - \beta_3 T, \tag{12}$$

$$t_{\theta\theta} = C_{12}e_{rr} + C_{11}e_{\theta\theta} + C_{13}e_{zz} - \beta_1 T, \tag{13}$$

where

$$e_{rz} = \frac{1}{2}\left(\frac{\partial u}{\partial z} + \frac{\partial w}{\partial r}\right), e_{rr} = \frac{\partial u}{\partial r}, e_{\theta\theta} = \frac{u}{r}, e_{zz} = \frac{\partial w}{\partial z},$$

$$T = \varphi - a_1\left(\frac{\partial^2\varphi}{\partial r^2} + \frac{1}{r}\frac{\partial\varphi}{\partial r}\right) - a_3\frac{\partial^2\varphi}{\partial z^2},$$

$$\beta_1 = \left(C_{11} + C_{12}\right)\alpha_1 + C_{13}\alpha_{3,}$$

$$\beta_3 = 2C_{13}\alpha_1 + C_{33}\alpha_3.$$

To facilitate the solution, the following dimensionless quantities are introduced:

$$\begin{aligned} &r' = \frac{r}{L}, z' = \frac{z}{L}, t' = \frac{C_1}{L}t, u' = \frac{\rho c_1^2}{L\beta_1 T_0}u, w' = \frac{\rho C_1^2}{L\beta_1 T_0}w,\\ &T' = \frac{T}{T_0}, t_{zr}' = \frac{t_{zr}}{\beta_1 T_0}, t_{zz}' = \frac{t_{zz}}{\beta_1 T_0}, t_{rr}' = \frac{t_{rr}}{\beta_1 T_0},\\ &\varphi' = \frac{\varphi}{T_0}, a_1' = \frac{a_1}{L^2}, a_3' = \frac{a_3}{L^2}. \end{aligned} \tag{14}$$

Let us take the Laplace and Hankel transforms defined by

$$f^*(r,z,s) = \int_0^\infty f(r,z,t)e^{-st}dt, \tag{15}$$

$$\tilde{f}(\xi,z,s) = \int_0^\infty f^*(r,z,s)rJ_n(r\xi)dr. \tag{16}$$

Using dimensionless quantities defined in (14) in Eqs. (7)–(13) and by suppressing the primes and applying (15) and (16) on the resulting quantities, we get

$$\begin{aligned} &\left(-\xi^2 - s^2 + \delta_2 D^2\right)\tilde{u} + (1-\xi)\delta_1 D\tilde{w}\\ &\quad + \left(-(1-\xi)\left(1 - a_3D^2\right) + a_1\xi^3\right)\tilde{\varphi} = 0, \end{aligned} \tag{17}$$

$$(1-\xi)\delta_1 D\tilde{u} + \left(\delta_3 D^2 - \xi^2\delta_2 - s^2\right)\tilde{w} - \frac{\beta_3}{\beta_1}D\left(1 + \xi^2 a_1 - a_3D^2\right)\tilde{\varphi} = 0, \tag{18}$$

$$\begin{aligned} &-\delta_6 s^2(1-\xi)\tilde{u} - \frac{\beta_3}{\beta_1}\delta_6 s^2 D\tilde{w} - \left(\delta_7 s^2\left(1 + \xi^2 a_1 - a_3D^2\right)\right.\\ &\left.\quad + \xi^2\left(K_1 + \delta_4 s\right) - D^2\left(K_3 + \delta_5 s\right)\right)\tilde{\varphi} = 0, \end{aligned} \tag{19}$$

where

$$\delta_1 = \frac{C_{13} + C_{44}}{C_{11}}, \delta_2 = \frac{C_{44}}{C_{11}}, \delta_3 = \frac{C_{33}}{C_{11}}, \delta_4 = \frac{K_1^* C_1}{L},$$

$$\delta_5 = \frac{K_3^* C_1}{L}, \delta_6 = -(1+G)\frac{T_0\beta_1^2}{\rho},$$

$$\delta_7 = -(1+G)\rho C_E C_1^2,$$

$$\mathrm{G} = \frac{1}{\chi}\left[\left(1 - \mathrm{e}^{-s\chi}\right)\left(1 - \frac{2\beta}{\chi s} + \frac{2\alpha^2}{\chi^2 s^2}\right) - \left(\alpha^2 - 2\beta + \frac{2\alpha^2}{\chi s}\right)\mathrm{e}^{-s\chi}\right].$$

$$\widetilde{t_{zz}} = \sum A_i(\xi,s)\eta_i cosh(q_i z) + \sum \mu_i A_i(\xi,s)\sinh\left(q_i z\right), \tag{20}$$

$$\widetilde{t_{rz}} = \sum A_i(\xi,s)d_i cosh(q_i z) + \xi\sum A_i(\xi,s)q_i sinh(q_i z), \tag{21}$$

$$\widetilde{t_{rr}} = \sum A_i(\xi,s)R_i cosh(q_i z) + \sum S_i A_i(\xi,s)\sinh\left(q_i z\right), \tag{22}$$

$$\widetilde{t_{\theta\theta}} = \sum A_i(\xi,s)M_i cosh(q_i z) + \sum N_i A_i(\xi,s)\sinh\left(q_i z\right), \tag{23}$$

where

$$\eta_i = \delta_9\xi - \frac{\beta_3}{\beta_1}\left(1 + a_1\xi^2\right)\mathrm{l_i} - \frac{\beta_3}{\beta_1}\mathrm{a_3 l_i q_i^2},$$

$$\mu_i = \left(\delta_9 + \delta_3 d_i\right)q_i,$$

$$M_i = \left(1 + \frac{\xi}{2}\right) - \left(1 + a_1\xi^2\right)\mathrm{l_i} + \mathrm{a_3 l_i q_i^2},$$

$$N_i = \left(\delta_8 + \delta_9 d_i\right)q_i,$$

$$R_i = \delta_8\left(1 + \frac{\xi}{2}\right) - l_i\left(1 + a_1\xi^2\right) + \mathrm{a_3} l_i \mathrm{q_i^2},$$

$$S_i = q_i\left(1 + \delta_3 d_i\right), \quad i = 1,2,3.$$

The non-trivial solution of (17)–(19) yields

$$(AD^6 + BD^4 + CD^2 + E)(\tilde{u},\tilde{w},\tilde{\varphi}) = 0. \tag{24}$$

where

$$A = \delta_2\delta_3\zeta_8 - \zeta_{11}\delta_2\zeta_7,$$

$$B = \delta_2\zeta_5\zeta_8 + \delta_3\zeta_1\zeta_8 + \delta_2\delta_3\zeta_9 - \delta_2\zeta_7\zeta_{10} - \zeta_7\zeta_1\zeta_{11} - \zeta_2^2\zeta_8 + \zeta_2\zeta_6\zeta_{11} + \zeta_4\zeta_7\zeta_2 - \delta_3\zeta_6\zeta_4,$$

$$C = \zeta_1\zeta_5\zeta_8 + \delta_2\zeta_9\zeta_5 + \delta_3\zeta_1\zeta_9 - \zeta_7\zeta_1\zeta_{10} - \zeta_2^2\zeta_9 + \zeta_2\zeta_6\zeta_{10} + \zeta_3\zeta_2\zeta_7 - \zeta_3\zeta_6\delta_3 - \zeta_4\zeta_6\zeta_5,$$

$$E = \zeta_5\zeta_1\zeta_9 - \zeta_6\zeta_5\zeta_3.$$

where $\zeta_1 = -\xi^2 - s^2$,

$\zeta_2 = \delta_1(1-\xi)$,

$\zeta_3 = a_1\xi^2 - (1-\xi)$,

$\zeta_4 = a_3(1-\xi)$,

$\zeta_5 = -s^2 - \xi^2\delta_2$,

$\zeta_6 = -\delta_6 s^2(1-\xi)$,

$\zeta_7 = -\delta_6 s^2\frac{\beta_3}{\beta_1}$,

$\zeta_8 = -(K_3 + \delta_5 s) + \delta_7 s^2 a_3$,

$\zeta_9 = -\delta_7 s^2(1 + a_1\xi^2) + \xi^2(K_1 + \delta_4 s)$,

$\zeta_{10} = -(1 + a_1\xi^2)\frac{\beta_3}{\beta_1}$,

$\zeta_{11} = a_3\frac{\beta_3}{\beta_1}$.

The solutions to Eq. (24)can be written in the form

$$\tilde{u} = \sum A_i(\xi,s)cosh(q_i z), \tag{25}$$

$$\tilde{w} = \sum d_i A_i(\xi,s)cosh(q_i z), \tag{26}$$

$$\tilde{\varphi} = \sum l_i A_i(\xi,s)cosh(q_i z). \tag{27}$$

where $A_i, i = 1,2,3$ being undetermined constants.and $\pm q_i (i = 1,2,3)$ are the roots of the Eq. (24) and d_i and l_i are given by

$$d_i = \frac{\delta_2\zeta_8 q_i^4 + (\zeta_8\zeta_1 - \zeta_4\zeta_6 + \delta_2\zeta_9)q_i^2 + \zeta_1\zeta_9 - \zeta_6\zeta_3}{(\delta_3\zeta_8 - \zeta_7\zeta_{11})q_i^4 + (\delta_3\zeta_9 + \zeta_5\zeta_8 - \zeta_7\zeta_{10})q_i^2 + \zeta_5\zeta_9},$$

$$l_i = \frac{\delta_2\delta_3 q_i^4 + (\delta_2\zeta_5 + \zeta_1\delta_3 - \zeta_2^2)q_i^2 + \zeta_1\zeta_5}{(\delta_3\zeta_8 - \zeta_7\zeta_{11})q_i^4 + (\delta_3\zeta_9 + \zeta_5\zeta_8 - \zeta_7\zeta_{10})q_i^2 + \zeta_5\zeta_9}.$$

4 Boundary conditions

We consider a stress-free surface at z = ± b, a cubical thermal source and normal force of unit magnitude is applied [3]. Mathematically, these can be written as

$$\frac{\partial\varphi}{\partial z} = \pm g_o F(r,z), \tag{28}$$

$$t_{zz}(r,z,t) = f(r,t), \tag{29}$$

$$t_{rz}(r,z,t) = 0. \tag{30}$$

By putting the values $\tilde{\varphi}, \widetilde{t_{zz}}, \widetilde{t_{rz}}$ from (20)–(20) and (27) in boundary conditions (28)–(30) and applying Hankel transform on the resulting equations yields

$$\sum A_i(\xi,s)l_i q_i \vartheta_i = \pm g_o\tilde{F}(\xi,z), \tag{31}$$

$$\sum A_i(\xi,s)\eta_i\theta_i + \sum \mu_i A_i(\xi,s)\vartheta_i = \tilde{f}(\xi,s), \tag{32}$$

$$\sum A_i(\xi,s)\left(\delta_2 q_i\vartheta_i + (1-\xi)l_i\theta_i\right) = 0. \tag{33}$$

Solving (31)–(33) for A_i, and putting in (25)–(27) and (20)–(23)we obtain the various components of displacement, stresses, and conductive temperature as

$$\begin{aligned}\tilde{u} = {} & \frac{\tilde{f}(\xi,s)}{\Delta}\{-[G_2G_9 - G_8G_3]\theta_1 + [G_1G_9 - G_7G_3]\theta_2 \\ & -[G_1G_8 - G_2G_7]\theta_3\} \\ & + \frac{g_o\tilde{F}(\xi,z)}{\Delta}\{[G_5G_9 - G_8G_6]\theta_1 - [G_4G_9 - G_6G_7]\theta_2 \\ & +[G_4G_8 - G_5G_7]\theta_3\}\end{aligned} \tag{34}$$

$$\tilde{w} = \frac{\tilde{f}(\xi,s)}{\Delta}\left\{-\left[G_2G_9 - G_8G_3\right]d_1\theta_1 + \left[G_1G_9 - G_7G_3\right]d_2\theta_2 - \left[G_1G_8 - G_2G_7\right]d_3\theta_3\right\} + \frac{g_o\tilde{F}(\xi,z)}{\Delta}\left\{\left[G_5G_9 - G_8G_6\right]d_1\theta_1 - \left[G_4G_9 - G_6G_7\right]d_2\theta_2 + \left[G_4G_8 - G_5G_7\right]d_3\theta_3\right\} \tag{35}$$

$$\tilde{\varphi} = \frac{\tilde{f}(\xi,s)}{\Delta}\left\{-\left[G_2G_9 - G_8G_3\right]l_1\theta_1 + \left[G_1G_9 - G_7G_3\right]l_2\theta_2 - \left[G_1G_8 - G_2G_7\right]l_3\theta_3\right\} + \frac{g_o\tilde{F}(\xi,z)}{\Delta}\left\{\left[G_5G_9 - G_8G_6\right]l_1\theta_1 - \left[G_4G_9 - G_6G_7\right]l_2\theta_2 + \left[G_4G_8 - G_5G_7\right]l_3\theta_3\right\} \tag{36}$$

$$\widetilde{t_{zz}} = \frac{\tilde{f}(\xi,s)}{\Delta}\left\{-\left[G_2G_9 - G_8G_3\right]\left(\eta_1\theta_1 + \mu_1\vartheta_1\right) + \left[G_1G_9 - G_7G_3\right]\left(\eta_2\theta_2 + \mu_2\vartheta_2\right) - \left[G_1G_8 - G_2G_7\right]\left(\eta_3\theta_3 + \mu_3\vartheta_3\right)\right\} + \frac{g_o\tilde{F}(\xi,z)}{\Delta}\left\{\left[G_5G_9 - G_8G_6\right]\left(\eta_1\theta_1 + \mu_1\vartheta_1\right) - \left[G_4G_9 - G_6G_7\right]\left(\eta_2\theta_2 + \mu_2\vartheta_2\right) + \left[G_4G_8 - G_5G_7\right]\left(\eta_3\theta_3 + \mu_3\vartheta_3\right)\right\} \tag{37}$$

$$\widetilde{t_{zr}} = \frac{\tilde{f}(\xi,s)}{\Delta}\left\{-\left[G_2G_9 - G_8G_3\right]\left(l_1(1-\xi)\theta_1 + \delta_2q_1\vartheta_1\right) + \left[G_1G_9 - G_7G_3\right]\left(l_2(1-\xi)\theta_2 + \delta_2q_2\vartheta_2\right) - \left[G_1G_8 - G_2G_7\right]\left(l_3(1-\xi)\theta_3 + \delta_2q_3\vartheta_3\right)\right\} + \frac{g_o\tilde{F}(\xi,z)}{\Delta}\left\{\left[G_5G_9 - G_8G_6\right]\left(l_1(1-\xi)\theta_1 + \delta_2q_1\vartheta_1\right) - \left[G_4G_9 - G_6G_7\right]\left(l_2(1-\xi)\theta_2 + \delta_2q_2\vartheta_2\right) + \left[G_4G_8 - G_5G_7\right]l_3(1-\xi)\theta_3 + \delta_2q_3\vartheta_3)\right\} \tag{38}$$

$$\widetilde{t_{rr}} = \frac{\tilde{f}(\xi,s)}{\Delta}\left\{-\left[G_2G_9 - G_8G_3\right]\left(R_1\theta_1 + S_1\vartheta_1\right) + \left[G_1G_9 - G_7G_3\right]\left(R_2\theta_2 + S_2\vartheta_2\right) - \left[G_1G_8 - G_2G_7\right]\left(R_3\theta_3 + S_3\vartheta_3\right)\right\} + \frac{g_o\tilde{F}(\xi,z)}{\Delta}\left\{\left[G_5G_9 - G_8G_6\right]\left(R_1\theta_1 + S_1\vartheta_1\right) - \left[G_4G_9 - G_6G_7\right]\left(R_2\theta_2 + S_2\vartheta_2\right) + \left[G_4G_8 - G_5G_7\right]((R_3\theta_3 + S_3\vartheta_3)\right\} \tag{39}$$

where

$$\Delta = G_1\left[G_5G_9 - G_8G_6\right] - G_2\left[G_4G_9 - G_6G_7\right] + G_3\left[G_4G_8 - G_5G_7\right]$$

$$\Delta_1 = -\tilde{f}(\xi,s)\left[G_2G_9 - G_8G_3\right] + g_o\tilde{F}(\xi,z)\left[G_5G_9 - G_8G_6\right]$$

$$\Delta_2 = \tilde{f}(\xi,s)\left[G_1G_9 - G_7G_3\right] - g_o\tilde{F}(\xi,z)\left[G_4G_9 - G_6G_7\right]$$

$$\Delta_3 = -\tilde{f}(\xi,s)\left[G_1G_8 - G_2G_7\right] + g_o\tilde{F}(\xi,z)\left[G_4G_8 - G_5G_7\right]$$

$$G_i = l_iq_i\vartheta_i,$$

$$G_{i+3} = \eta_i\theta_i + \mu_i\vartheta_i,$$

$$G_{i+6} = \delta_2q_i\vartheta_i + (1-\xi)l_i\theta_i,$$

$$\cosh\left(q_iz\right) = \theta_i, \quad \sinh\left(q_iz\right) = \vartheta_i, \quad i = 1,2,3.$$

5 Applications

As an application of the problem, we take the source functions as

$$F(r,z) = z^2e^{-\omega r}, \tag{40}$$

$$f(r,t) = \frac{1}{2\pi r}\delta(ct-r). \tag{41}$$

where δ (ct − r) is the Dirac delta function.

Applying Laplace and Hankel Transform, on Eqs. (40)–(41), gives

$$\tilde{F}(\xi,z) = \frac{z^2\omega}{\left(\xi^2+\omega^2\right)^{\frac{3}{2}}}, \tag{42}$$

$$\tilde{f}(\xi,s) = \frac{1}{2\pi\sqrt{\xi^2 + \frac{s}{c^2}^2}} \tag{43}$$

6 Inversion of the transforms

In order to obtain the solution in the physical domain, the transforms in Eqs. (34)-(39) has to be inverted. For this, first, we will invert the Hankel transform by

$$f(r,z,t) = \int_0^\infty \xi \tilde{f}(\xi,z,s) J_n(\xi r) d\xi. \quad (44)$$

The method for evaluating this integral is described in Press et al.[28].

7 Particular cases

(i) If we take $K_{ij}^* \neq 0$, Eq. (3) is GN-III theory or GN theory with energy dissipation.
(ii) Equation (3) becomes GN-II theory or GN theory without energy dissipation if we take $K_{ij}^* = 0$,
(iii) If we take $K_{ij} = 0$ the equation of the GN theory of type III reduces to the GN theory of type I, which is identical to the classical theory of thermoelasticity.

8 Numerical results and discussion

This section presents numerical results that illustrate the theoretical results and the effects of MDD. The material properties of transversely isotropic cobalt has been chosen for the numerical calculation. According to [29], the physical information for a single cobalt crystal is provided by

$C_{11} = 3.07 \times 10^{11}\ \mathrm{Nm}^{-2}$,

$C_{12} = 1.650 \times 10^{11}\ \mathrm{Nm}^{-2}$,

$C_{13} = 1.027 \times 10^{10}\ \mathrm{Nm}^{-2}$,

$C_{33} = 3.581 \times 10^{11}\ \mathrm{Nm}^{-2}$

$C_{44} = 1.510 \times 10^{11}\ \mathrm{Nm}^{-2}$,

$C_E = 4.27 \times 10^2 \mathrm{j\ Kg}^{-1}\ \mathrm{deg}^{-1}$,

$\beta_1 = 7.04 \times 10^6\ \mathrm{Nm}^{-2}\ \mathrm{deg}^{-1}$, $\rho = 8.836 \times 10^3\ \mathrm{Kg\ m}^{-3}$

$\beta_3 = 6.90 \times 10^6\ \mathrm{Nm}^{-2}\ \mathrm{deg}^{-1}$,

$K_1 = 0.690 \times 10^2\ \mathrm{Wm}^{-1}\ \mathrm{Kdeg}^{-1}$, $K_3 = 0.690 \times 10^2\ \mathrm{Wm}^{-1}\ \mathrm{K}^{-1}$,

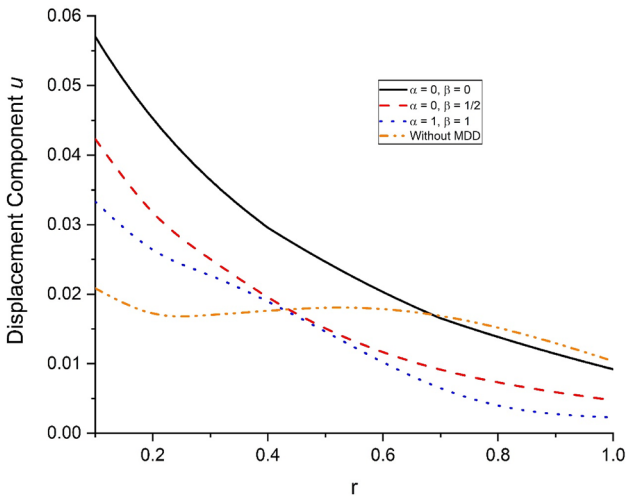

Fig. 1 Variations of displacement component u with radius r

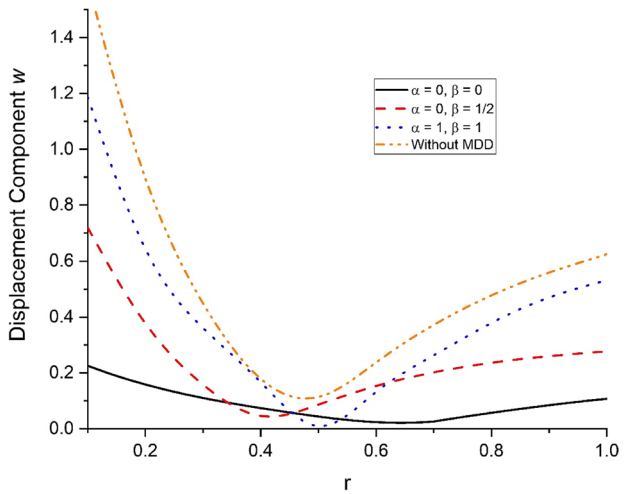

Fig. 2 Variations of displacement component *w* with radius r

$K_1^* = 0.02 \times 10^2\ \mathrm{NSec}^{-2}\ \mathrm{deg}^{-1}$,

$K_3^* = 0.04 \times 10^2\ \mathrm{NSec}^{-2}\ \mathrm{deg}^{-1}$.

The values of normal force stress t_{zz}, tangential stress t_{zr}, radial stress t_{rr}, and conductive temperature φ for a transversely isotropic thermoelastic solid with two temperature is illustrated graphically to demonstrate the effect of MDD.

(i) The solid black line corresponds to $K(t-\xi) = 1$ when $\alpha = 0, \beta = 0$,
(ii) The dashed red line corresponds to $K(t-\xi) = \xi - t + 1$when $\alpha = 0, \beta = \frac{\chi}{2}$,

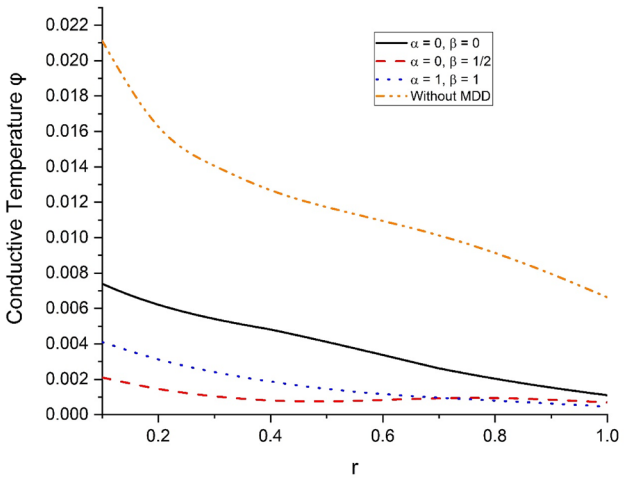

Fig. 3 Variations of conductive temperature φ w.r.t. radius r

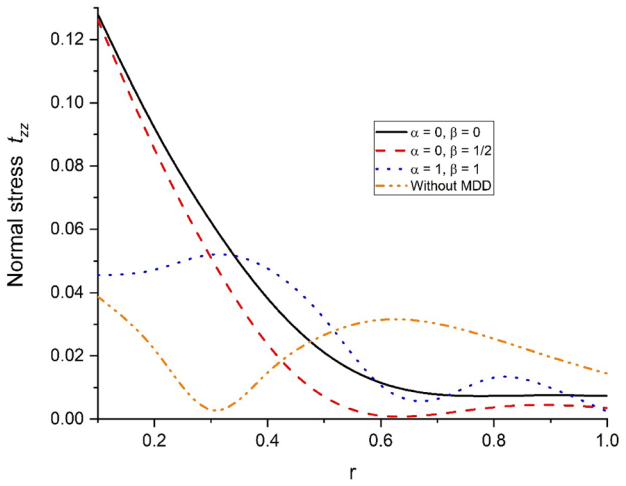

Fig. 5 Variations of normal stress t_{zz} with radius r

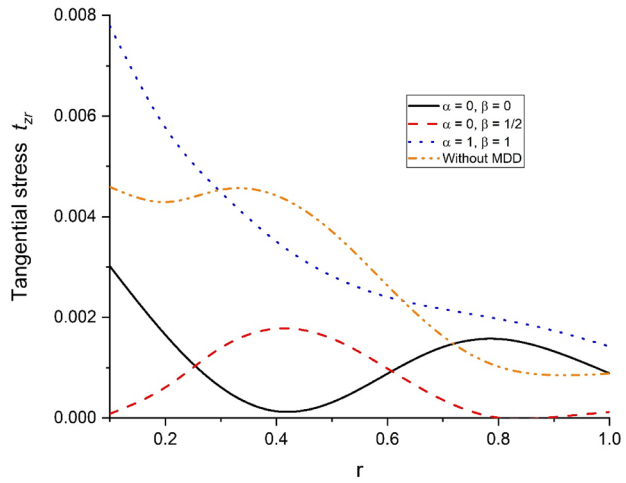

Fig. 4 Variations of tangential stress t_{zr} with radius r

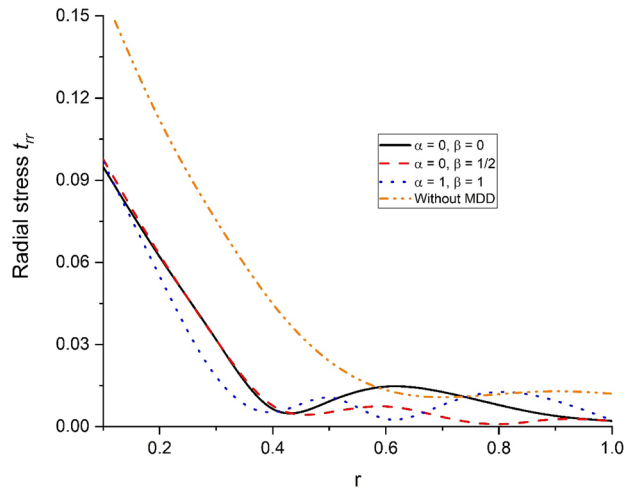

Fig. 6 Variations of radial stress t_{rr} with radius r

(iii) The dotted blue line corresponds to $K(t-\xi) = \left[1 + \frac{(\xi - t)}{\chi}\right]^2$ when $\alpha = 1, \beta = 1$.
(iv) The dash-dot yellow line corresponds to without MDD.

Figure 1 exhibits the displacement component w w.r.t.r for various values of the kernel function of MDD. The variation in the displacement component sharply decreases with the change in the radius of the thick circular plate. The kernel function $K(t-\xi) = 1$ when $\alpha = 0, \beta = 0$ shows the higher variation near the interface and starts vanishing towards the outer surface of the thick circular plate. However kernel function $K(t-\xi) = \left[1 + \frac{(\xi - t)}{\chi}\right]^2$ when $\alpha = 1, \beta = 1$ reduces the variation in the displacement component. So lower the value of the kernel function higher the variation in the displacement component. Moreover, the displacement component shows the opposite behavior without MDD.

Figure 2 depicts the values of displacement component w w.r.t.r for various values of the kernel function of MDD. The variation in the displacement component sharply decreases with the change of radius of the thick circular plate till the half value of r and then there is a rise in the value of w. The kernel function $K(t-\xi) = 1$ when $\alpha = 0, \beta = 0$ shows the minimum variation near the interface and starts vanishing towards the outer surface of the thick circular plate. However kernel function $K(t-\xi) = \left[1 + \frac{(\xi - t)}{\chi}\right]^2$ when $\alpha = 1, \beta = 1$increases the variation in the displacement component. So lower the value

of the kernel function lowers the variation in the displacement component. Moreover, the displacement component shows the maximum variation without MDD.

Figure 3 demonstrates the variations of conductive temperature φ w.r.t.r for various values of the kernel function of MDD. The variation in the φ sharply decreases with the change in the radius of the thick circular plate. The kernel function $K(t-\xi)=1$ when $\alpha=0,\beta=0$ shows the higher variation near the interface but away from the loading surface, it follows remains constant near the zero value. However kernel function $K(t-\xi)=\left[1+\frac{(\xi-t)}{\chi}\right]^2$ when $\alpha=1,\beta=1$ reduces the variation in the φ. So lower the value of the kernel function higher the variation in the φ. Moreover, the φ shows the maximum value without MDD.

Figure 4 illustrates the variations of tangential stress t_{zr} w.r.t.r for various values of the kernel function of MDD. In the initial range of distance r, the value of t_{zr} follow an oscillatory pattern for all the various values of the kernel function of MDD. The kernel function $K(t-\xi)=1$ when $\alpha=0,\beta=0$ shows the lowest variation near the interface but away from the loading surface, it follows remains constant near the zero value. However kernel function $K(t-\xi)=\left[1+\frac{(\xi-t)}{\chi}\right]^2$ when $\alpha=1,\beta=1$ maximizes the variation in the t_{zr}. So higher the value of the kernel function higher the variation in the t_{zr}.

Figure 5 shows the variations of normal stress t_{zz} w.r.t.r for various values of the kernel function of MDD. In the initial range of distance r, the value of t_{zz} follow an oscillatory pattern for all the various values of the kernel function of MDD. The kernel function $K(t-\xi)=1$when $\alpha=0,\beta=0$ shows the lowest variation near the interface but away from the loading surface, it follows remains constant near the zero value. However kernel function $K(t-\xi)=\left[1+\frac{(\xi-t)}{\chi}\right]^2$ when $\alpha=1,\beta=1$ maximizes the variation in the t_{zz}. So lower the value of the kernel function higher the variation in the t_{zz}.

Figure 6 shows the variations of radial stress t_{rr} w.r.t.r for various values of the kernel function of MDD. In the initial range of distance r, there is a sharp decrease in the value of radial stress t_{rr} with distance r various values of the kernel function of MDD then the variations are very small owing to the scale of the graph and the kernel function $K(t-\xi)=1$when $\alpha=0,\beta=0$ shows the highest variation near the interface but away from the loading surface, it follows remains constant near the zero value. However kernel function $K(t-\xi)=\left[1+\frac{(\xi-t)}{\chi}\right]^2$ when $\alpha=1,\beta=1$ minimize the variation in the t_{rr}. So lower the value of the kernel function higher the variation in the t_{rr}.

9 Conclusions

Transversely isotropic thick circular plates with ring loads are investigated in the present study. The modified Green Nagdhi heat conduction equation with & without energy dissipation by introducing memory-dependent derivatives with two temperatures has been used to model the problem. From the graphs, it is clear that there is a momentous effect of isotropy on the deformation of various components of displacement, stresses, temperature change, and conducive temperature. The effect of the kernel function of MDD theory has an imperative impact on the investigation of the deformation of the body. As distance r varied from the point of application of the load source, sharp decrease in the values of all the characteristics quantities of the thick plate. It is seen that as the disturbances travel through different constituents of the medium, the variations of t_{zz}, $t_{zr,}$ and φ, it experiences abrupt shifts, resulting in an erratic/uniform pattern of curves. The trend of curves demonstrates how the MDD theory affects the medium and fits the necessary criteria for the investigation. Kernel function $K(t-\xi)=\left[1+\frac{(\xi-t)}{\chi}\right]^2$ when $\alpha=1,\beta=1$ decreases the variation in the displacement component, of t_{zz}, $t_{zr,}$ and φ. The outcomes of this research are exceptionally valuable in the 2-D problem of the dynamic response of GN-III theory with MDD in transversely isotropic thermoelastic solid with two temperature which has numerous geophysical and industrialized uses. The findings from this study are helpful in engineering issues, notably in determining the condition of stresses in a thick circular plate that has experienced internal transient heat.

Acknowledgements Not applicable.

Author contributions IK: Idea formulation, conceptualization, formulated strategies for mathematical modelling, methodology refinement, formal analysis, validation, writing—review and editing. KS: conceptualization, effective literature review, experiments and simulation, investigation, methodology, software, supervision, validation, visualization, writing—original draft. Both authors read and approved the final manuscript.

Funding No fund/grant/scholarship has been taken for the research work.

Availability of data and materials For the numerical results, silicon material has been taken from [29].

Declarations

Conflict of interest The authors declare that they have no conflict of interest.

References

1. Duhamel JM (1938) Memories of the molecular actions developed by changes in temperatures in solids. Mummy Div Sav (AcadSci Par) 5:440–498
2. Sharma N, Kumar R, Lata P (2015) Disturbance due to inclined load in transversely isotropic thermoelastic medium with two temperatures and without energy dissipation. Mater Phys Mech 22:107–117
3. Kumar R, Sharma N, Lata P (2016) Effect of two temperatures and thermal phase-lags in a thick plate due to a ring load with axisymmetric heat supply. Comput Methods Sci Technol 22:153–162. https://doi.org/10.12921/cmst.2016.0000005
4. Tripathi JJ, Kedar GD, Deshmukh KC (2016) Generalized thermoelastic diffusion in a thick circular plate including heat source. Alex Eng J 55:2241–2249. https://doi.org/10.1016/j.aej.2016.06.003
5. Kant S, Mukhopadhyay S (2017) A detailed comparative study on responses of four heat conduction models for an axisymmetric problem of coupled thermoelastic interactions inside a thick plate. Int J Therm Sci 117:196–211. https://doi.org/10.1016/j.ijthermalsci.2017.03.018
6. Kant S, Mukhopadhyay S (2019) An investigation on responses of thermoelastic interactions in a generalized thermoelasticity with memory-dependent derivatives inside a thick plate. Math Mech Solids 24:2392–2409. https://doi.org/10.1177/1081286518755562
7. Youssef HM (2011) Theory of two-temperature thermoelasticity without energy dissipation. J Therm Stress 34:138–146. https://doi.org/10.1080/01495739.2010.511941
8. Lata P (2018) Fractional order thermoelastic thick circular plate with two temperatures in frequency domain. Appl Appl Math Int J 13:1216–1229
9. Galović S, Popović M, Todorović DM (2010) Photothermal dynamic elastic bending in a semiconductor circular plate induced by a focused laser beam. J Phys Conf Ser 214:012113. https://doi.org/10.1088/1742-6596/214/1/012113
10. Senjanović I, Hadžić N, Vladimir N, Cho DS (2014) Natural vibrations of thick circular plate based on the modified Mindlin theory. Arch Mech 66:389–409
11. Kumar R, Kaushal S, Dahiya V (2021) Porosity and phase lags response of thick circular plate in modified couple stress thermoelastic medium. ZAMM J Appl Math Mech/Zeitschrift Für Angew Math Und Mech. https://doi.org/10.1002/zamm.202100098
12. Kumar R, Miglani A, Rani R (2018) Transient analysis of nonolocal microstretch thermoelastic thick circular plate with phase lags. Mediterr J Model Simul 09:25–42
13. Kaur I, Singh K (2021) Fractional order strain analysis in thick circular plate subjected to hyperbolic two temperature. Partial Differ Equ Appl Math 4:100130. https://doi.org/10.1016/J.PADIFF.2021.100130
14. Mallik SH, Kanoria M (2008) A two dimensional problem for a transversely isotropic generalized thermoelastic thick plate with spatially varying heat source. Eur J Mech A/Solids 27:607–621. https://doi.org/10.1016/j.euromechsol.2007.09.002
15. Hasheminejad SM, Rafsanjani A (2009) Three-dimensional vibration analysis of thick fgm plate strips under moving line loads. Mech Adv Mater Struct 16:417–428. https://doi.org/10.1080/15376490902781209
16. Kaur I, Singh K (2021) Effect of memory dependent derivative and variable thermal conductivity in cantilever nano-beam with forced transverse vibrations. Forces Mech 5:100043. https://doi.org/10.1016/j.finmec.2021.100043
17. Kaur I, Singh K (2022) Functionally graded nonlocal thermoelastic nanobeam with memory-dependent derivatives. SN Appl Sci 4:329. https://doi.org/10.1007/s42452-022-05212-8
18. Nasr ME, Abouelregal AE (2022) Light absorption process in a semiconductor infinite body with a cylindrical cavity via a novel photo-thermoelastic MGT model. Arch Appl Mech. https://doi.org/10.1007/S00419-022-02128-Y
19. Abouelregal AE, Moustapha MV, Nofal TA, Rashid S, Ahmad H (2021) Generalized thermoelasticity based on higher-order memory-dependent derivative with time delay. Results Phys 20:103705. https://doi.org/10.1016/j.rinp.2020.103705
20. Abouelregal AE, Sedighi HM, Sofiyev AH (2021) Modeling photo-excited carrier interactions in a solid sphere of a semiconductor material based on the photothermal Moore–Gibson–Thompson model. Appl Phys A 127:845. https://doi.org/10.1007/s00339-021-04971-2
21. Ezzat MA, El-Karamany AS, El-Bary AA (2014) Generalized thermo-viscoelasticity with memory-dependent derivatives. Int J Mech Sci 89:470–475. https://doi.org/10.1016/j.ijmecsci.2014.10.006
22. Ezzat MA, El-Karamany AS, El-Bary AA (2015) A novel magneto-thermoelasticity theory with memory-dependent derivative. J Electromagn Waves Appl 29:1018–1031. https://doi.org/10.1080/09205071.2015.1027795
23. Ezzat MA, El-Karamany AS, El-Bary AA (2016) Generalized thermoelasticity with memory-dependent derivatives involving two temperatures. Mech Adv Mater Struct 23:545–553. https://doi.org/10.1080/15376494.2015.1007189
24. Green AE, Naghdi PM (1993) Thermoelasticity without energy dissipation. J Elast 31:189–208. https://doi.org/10.1007/BF00044969
25. Wang J-L, Li H-F (2011) Surpassing the fractional derivative: concept of the memory-dependent derivative. Comput Math Appl 62:1562–1567. https://doi.org/10.1016/j.camwa.2011.04.028
26. Bachher M (2019) Plane harmonic waves in thermoelastic materials with a memory-dependent derivative. J Appl Mech Tech Phys 60:123–131. https://doi.org/10.1134/S0021894419010152
27. Slaughter WS (2002) The linearized theory of elasticity. Birkhäuser, Boston. https://doi.org/10.1007/978-1-4612-0093-2
28. Press WH, Teukolsky SA, Flannery BP (1980) Numerical recipes in Fortran. Cambridge University Press, Cambridge
29. Dhaliwal A, Singh RS (1980) Dynamic coupled thermoelasticity. Hindustan Publication Corporation, New Delhi